EFFECT OF LOADS ON THE STABILITY OF COHESIVE SLOPES IN UNDRAINED CONDITION

Dr. Mosa J. Al-Mosawe
Professor of Civil Engineering, Head of University of Baghdad

Dr. Mohammed Yousif Fattah
Lecturer, Building and Construction Eng. Department, University of Technology

ABSTRACT

The undrained stability of cohesive slopes ($\phi_u = 0$) subjected to surcharge loads is studied in this paper. Problems of this kind are involved in structures rapidly built near the crest of cohesive slopes and heavy equipment (e.g. draglines, buldozers and railways) move on slope. Using the non-linear finite element method, the effects of line loads and uniformly distributed loads are studied and the distribution of stresses under these loads is examined. The value of Pcr (critical line load) required equating the driving and resisting moments for a unit length of the slope was computed using the computer program. The process was repeated until a minimum Pcr was obtained.

الخلاصة

الاستقرارية غير المبزولة للمنحدرات الطينية ($\phi_u = 0$) المعرضة إلى أحمال مختلفة درست في هذا البحث. إن المسائل من هذا النوع مطلوبة في المنشات التي تنشأ سريعا قرب قمة المنحدرات الطينية وحالة المعدات الثقيلة (مثل الحفارات السلكية و البلدوزرات و خطوط السكك) التي تتحرك على المنحدر. باستعمال طريقة العناصر المحددة غير الخطية درست تأثيرات الأحمال الخطية و الأحمال الموزعة بانتظام و أختبر توزيع الإجهادات تحت هذه الأحمال. إن قيمة الحمل الخطي الحرجة المطلوبة لمعادلة كل من العزم المدور و العزم المقاوم لوحدة طول من المنحدر قد حسبت باستخدام برنامج حاسوبي. و قد كررت عملية الحساب مرات عديدة إلى أن تم الحصول إلى القيمة الدنيا للحمل الحرج.

KEY WORDS

Stability, slopes, finite elements, cohesive

INTRODUCTION

Despite its widespread use, the limit equilibrium stability analysis method is subjected to several theoretical shortcomings. This led to the development of the finite element method of stability analysis which eliminates most of the limitations found in limit equilibrium methods. Theoretical objections that apply in general to all limit equilibrium analysis methods, either total or effective stress, have been reported by Wright et al. (1973). These methods also have a number of common characteristics, (Adikari and Cummins, 1985).

Conventional methods of stability analysis are restricted to two-dimensional (plane strain) mode of failure. Baligh and Azzouz (1975 and 1977) studied two and three-dimensional effects on the stability of cohesive slopes and presented the effect of line loads in the form of charts and considered three-dimensional analysis for line loads of finite length.

Non-Linear Finite Element Method

This method consists of using the internal stresses determined by performing analyses of the slopes to determine, (Wright et al., 1973):

1- The variation of normal stress and factor of safety along the slip surface.
2- The overall factor of safety of each slope.

Eight-noded quadrilateral isoparametric plane strain elements are used. A computer program edited by Smith and Griffiths (1988) is used with the following changes:

1- The program was developed to consider different types of geometries and materials.
2- The initial stresses in the soil were taken into account. A procedure called "gravity turn-on analysis" which was improved by Dunlop and Duncan (1970) was used. In the plane strain case, the in situ stresses are calculated by considering the lateral earth pressure coefficient, k_o.
3- The program considers gravity loading only. It was modified to consider external loads too.

The problem to be analysed is a slope of Mohr-Coulomb failure criterion material subjected to gravity loading and external loads. The factor of safety (F) is defined as the proportion by which tan ϕ (angle of friction) and c (cohesion) must be reduced in order to cause failure.

The loads in this problem are applied in a single increment and a trial "factor of safety loop" is considered. The factored soil strength parameters for each factor of safety are obtained by dividing the strength parameters by the values of F. Keeping the loads constant, several values of F are attempted until the algorithm fails to converge. The stress-strain law involves visco-plastic material behaviour. For simplification, the yield and ultimate failure surfaces are considered identical.

The failure of a soil element in a clay layer is defined by:

$$F_E = \frac{2Cu}{\sigma_1 - \sigma_3} \leq 1$$

where $(\sigma_1-\sigma_3)$ is the deviator stress corresponding to the mobilized strain, (Matsuo and Kunio, 1977).

Effect of Line Loads

The value of Pcr (critical line load) required equating the driving and resisting moments for a unit length of the slope was computed using the computer program. The process was repeated until a minimum Pcr was obtained. The results of the analysis are shown in **Figs. (1) to (7).**

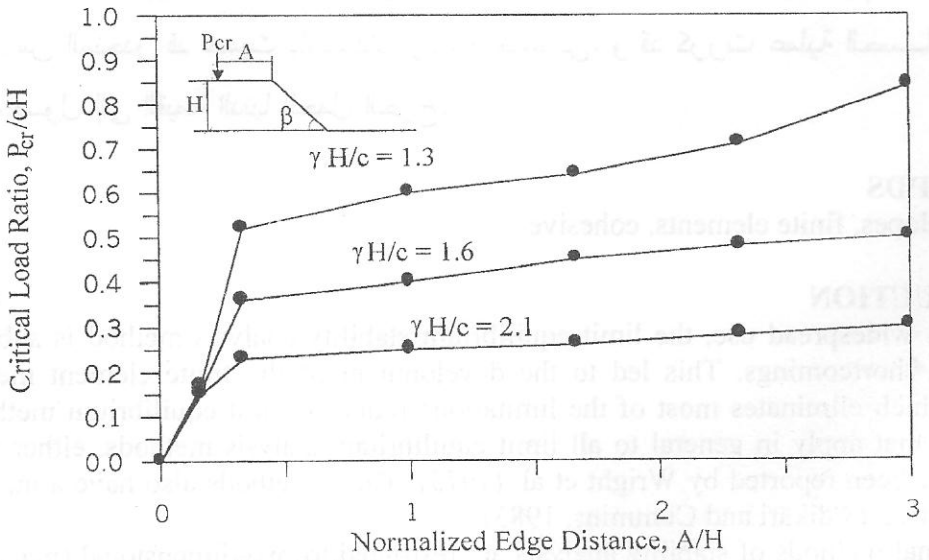

Fig. (1) – Stability chart for line loads, (slope 1:1).

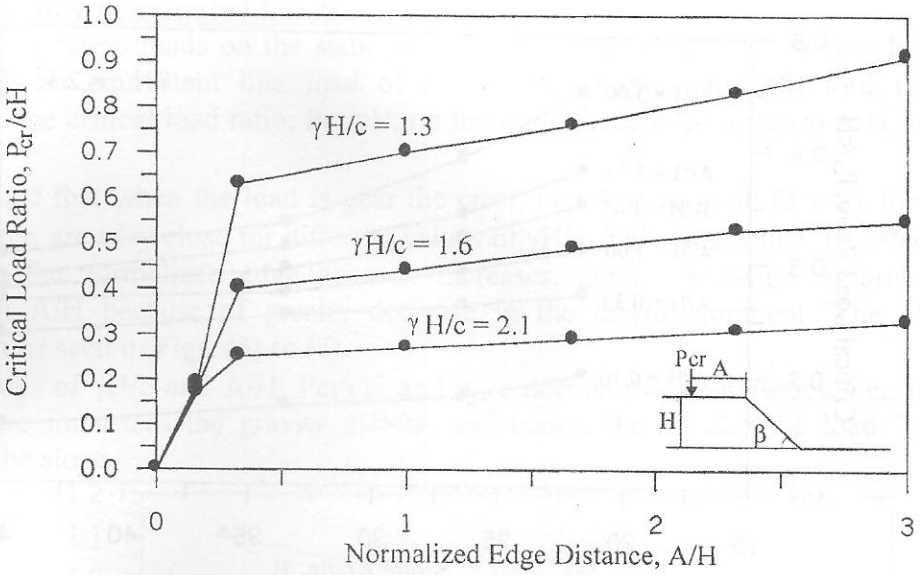

Fig. (2) – Stability chart for line loads, (slope 1.5:1).

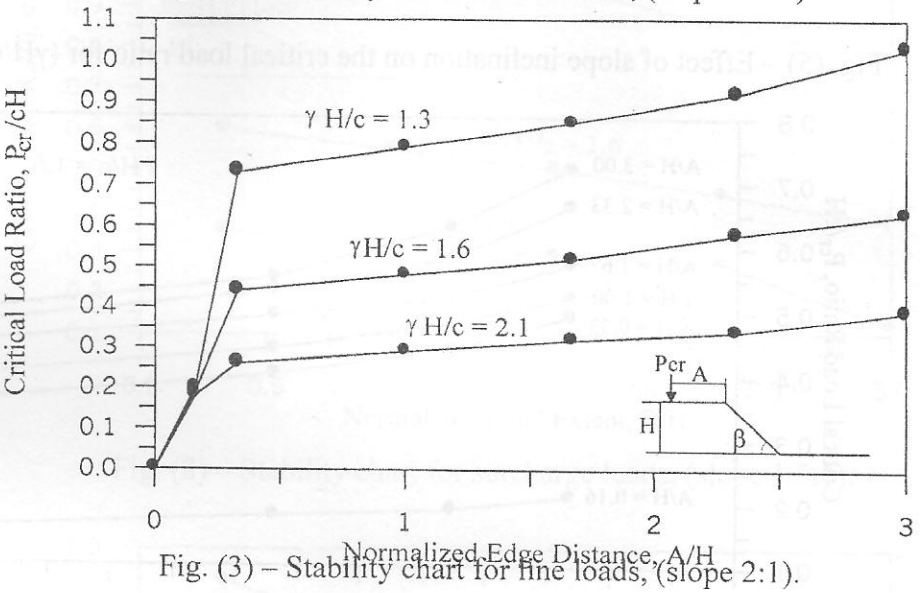

Fig. (3) – Stability chart for line loads, (slope 2:1).

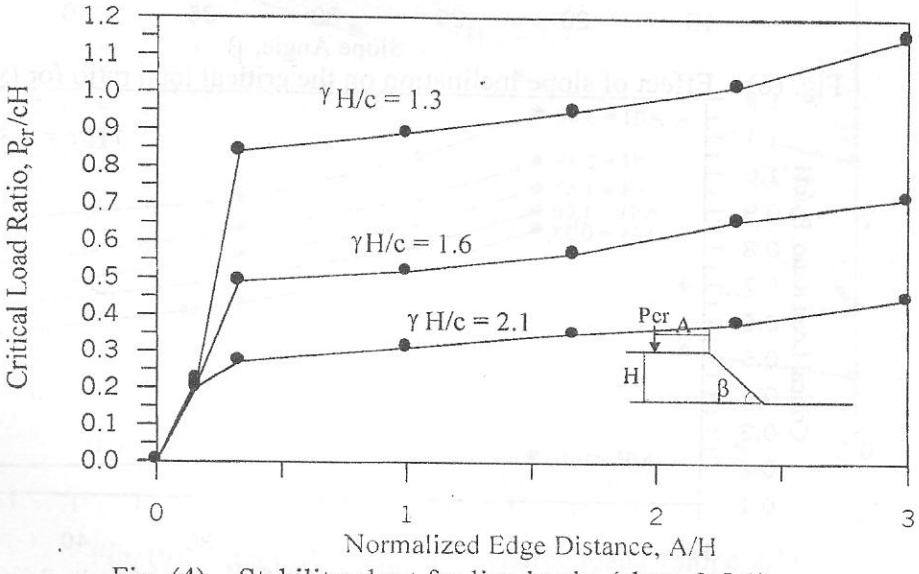

Fig. (4) – Stability chart for line loads, (slope 2.5:1).

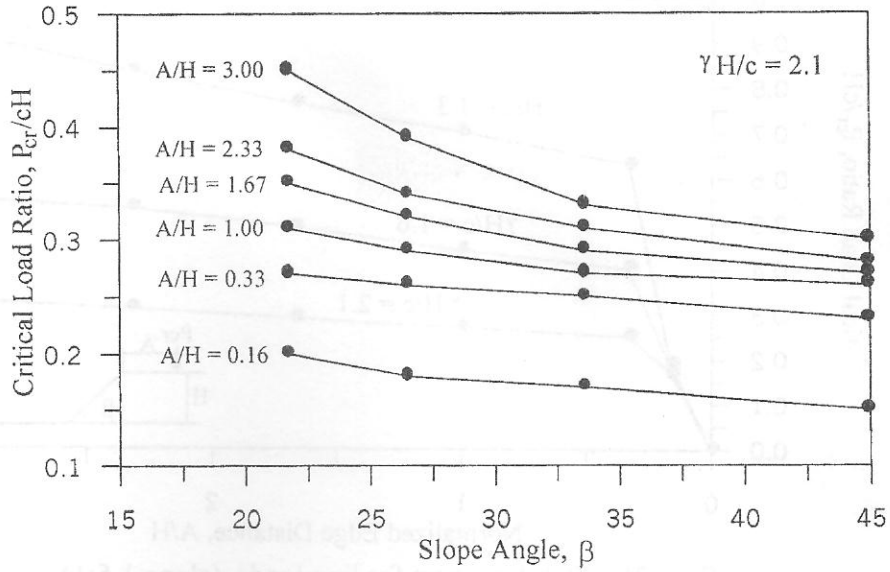

Fig. (5) – Effect of slope inclination on the critical load ratio for (γH/c = 2.1).

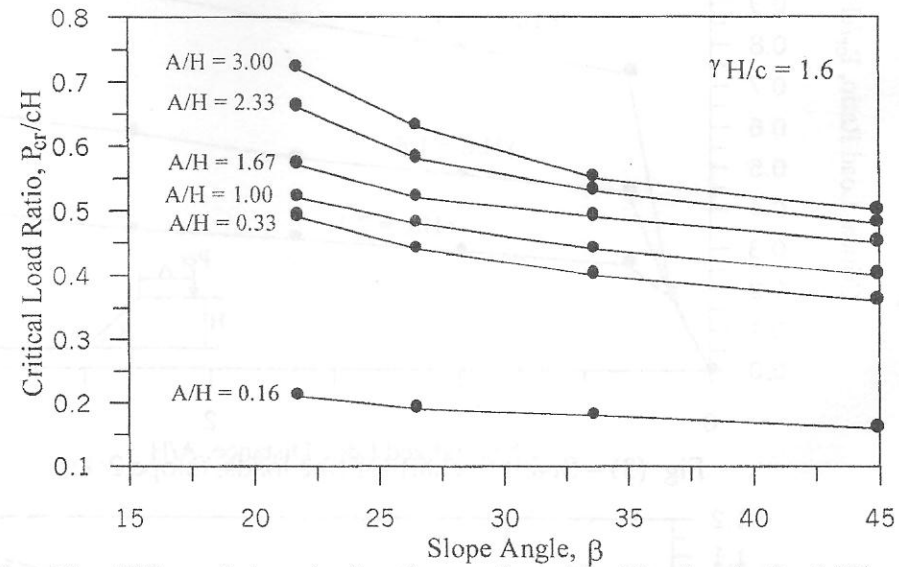

Fig. (6) – Effect of slope inclination on the critical load ratio for (γH/c = 1.6).

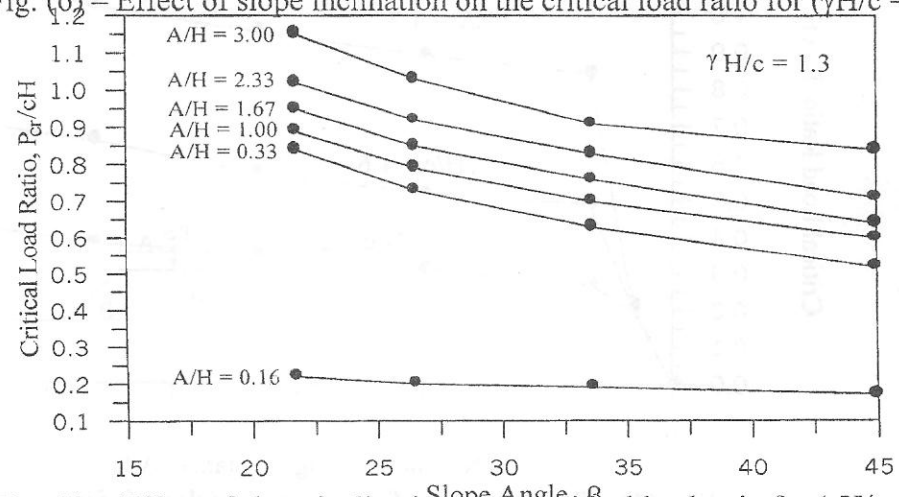

Fig. (7) – Effect of slope inclination on the critical load ratio for (γH/c = 1.3).

Effect of Uniformly Distributed Loads

The effect of surcharge loads on the stability is usually taken into consideration by replacing the surcharge with an equivalent line load of an infinite length. **Figs. (8) and (9)** present the dependence of the critical load ratio, Pcr/cH, on the normalized edge distance A/H for three values of (γH/c).

It can be noticed that when the load is near the crest, i.e., A/H is small ($\leq$ 0.2), the values of the critical load, Pcr, are very close for different values of γH/c. This means that the effect of gravity is negligible. As the normalized edge distance increases, gravity becomes important and Pcr/cH increases with A/H because of greater decrease in the driving moment. The effect of slope inclination can be seen in **Figs. (5) to (7).**

For given values of γH/c and A/H, Pcr/cH and q_{cr}/c decrease as β increases, i.e., the steeper the slope, the more important the gravity effects, and hence, the smaller the load Pcr that can be supported by the slope.

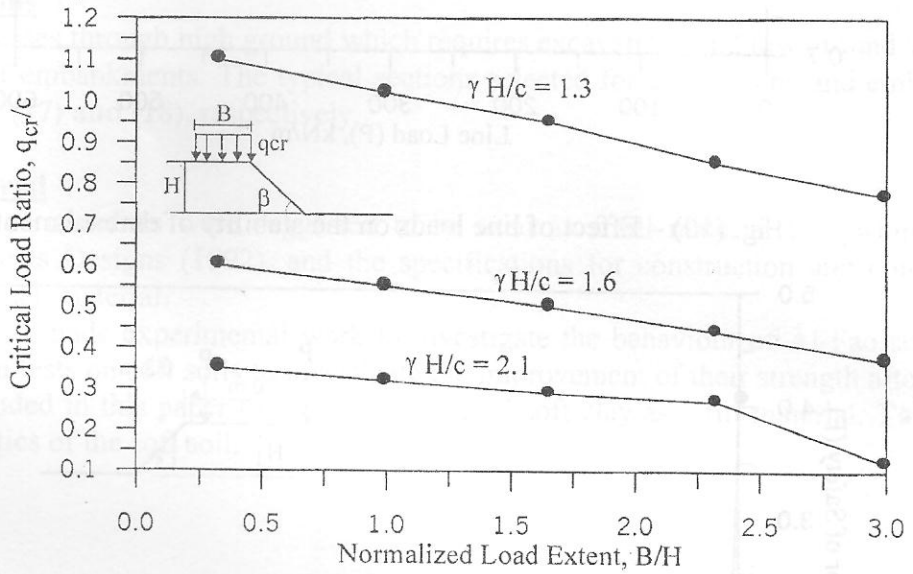

Fig. (8) – Stability chart for surcharge loads, (slope 1.5:1).

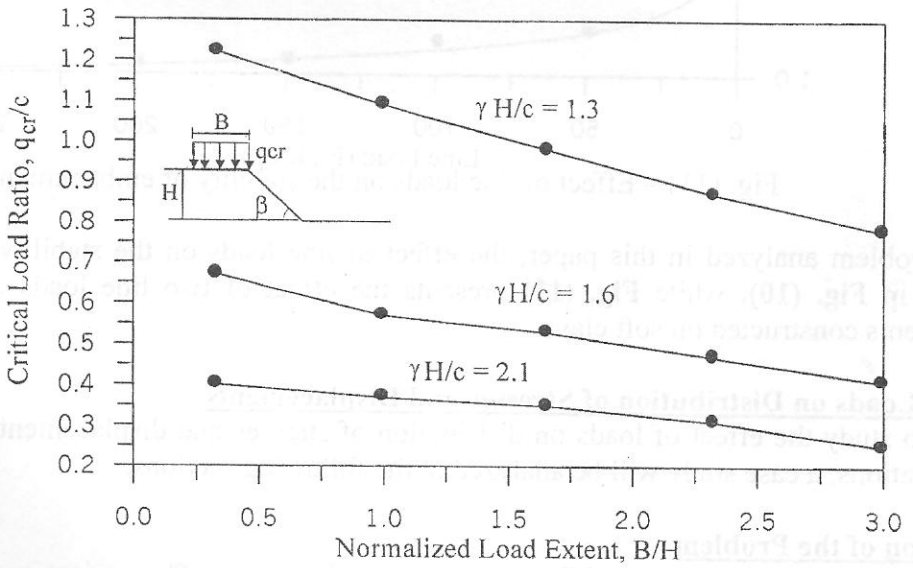

Fig. (9) – Stability chart for surcharge loads, (slope 2:1).

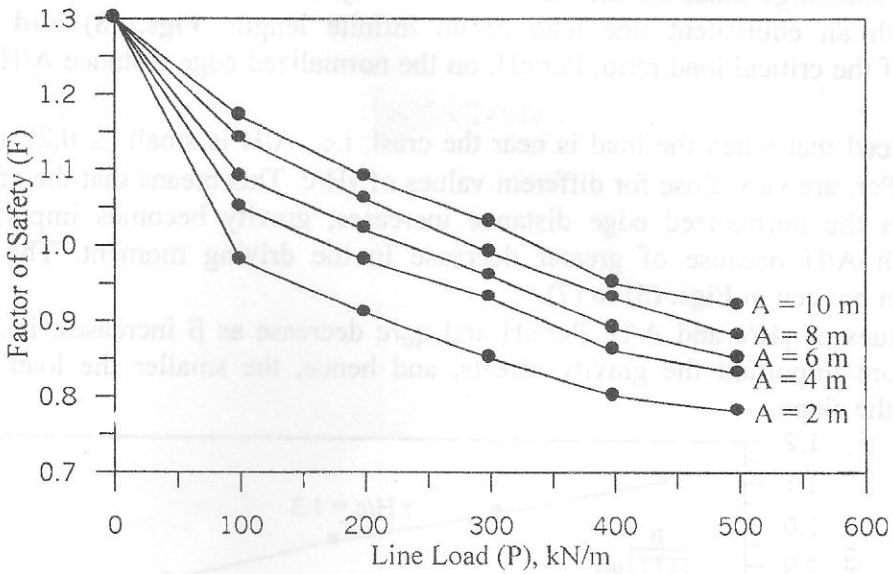

Fig. (10) – Effect of line loads on the stability of embankment.

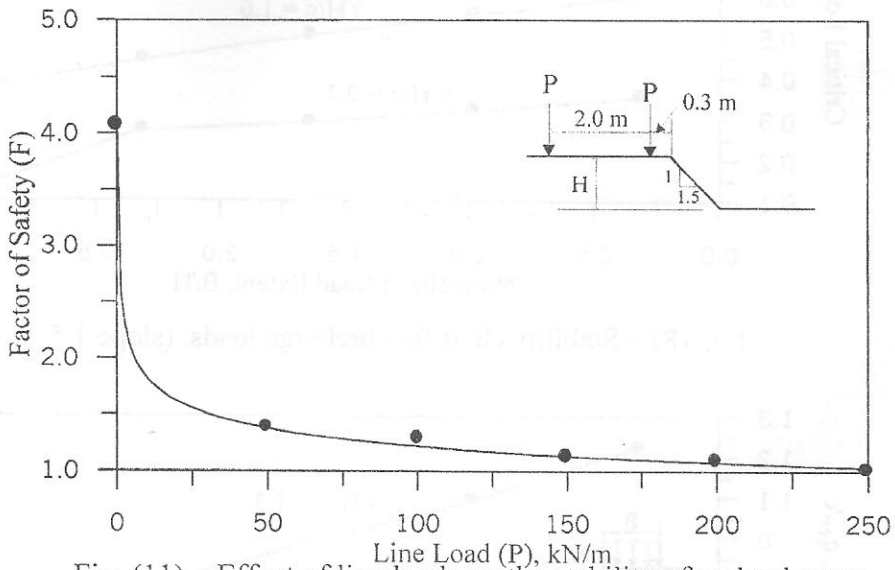

Fig. (11) – Effect of line loads on the stability of embankment.

For the problem analyzed in this paper, the effect of line loads on the stability of excavations is presented in **Fig. (10),** while **Fig. (11)** presents the effect of two line loads on the stability of embankments constructed on soft clays.

Effect of Loads on Distribution of Stresses and Displacements

In order to study the effect of loads on distribution of stresses and displacements in embankments and excavations, a case study will be analyzed in the following sections.

Description of the Problem

The problem was selected from Al-Basrah water supply project. The project consists of a channel about 200 km long starting from Al-Bada'a near Al-Nassiriya and passing through a region which was the old channel of Shatt Al-Arab. The site selected for this research lies at the interchange of the channel with Abu Skair at a place between Basrah universal airport and Shatt Al-Basrah.

The physical properties of the soil are presented in **Fig. (12).** According to the unified soil classification system, the soil is classified as CL; inorganic clay of low to medium plasticity. The site was investigated by the National Center for Construction Laboratories, (NCCL, 1992). Eighteen boreholes were drilled in the site, and detailed tests were made on disturbed and undisturbed samples.

Fig. (13) shows the distribution of the overburden pressure, σ'_{vo}, and preconsolidation pressure, σ'_{p}, with depth. **Fig. (14)** shows the variation of the overconsolidation ratio OCR with depth, while **Fig. (15)** shows the variation of the undrained shear strength, Cu, measured from triaxial tests with depth.

The variation of the undrained strength ratio (Cu/σ'_{vo}) with OCR is shown in **Fig. (16).**

The overconsolidation state of the clay was not caused by geological release, but may be caused by other factors such as aging effects, seepage forces and evaporation, (Hanzawa, 1977).

Typical Sections

The channel passes through high ground which requires excavations and low ground which requires construction of embankments. The typical sections selected for excavations and embankments are shown in **Figs. (17) and (18),** respectively.

The Fill Material

Several types of materials were suggested to be used as a fill material by Al-Furat Center for Irrigation Projects Designs (1992), and the specifications for construction and compaction were suggested for each material.

Al-Mufty (1990) made experimental work to investigate the behaviour of Al-Fao soil and carried out compaction tests on soft soils to investigate the improvement of their strength after compaction. It is recommended in this paper to use the compacted soft clay as a fill material. **Table (1)** shows the characteristics of the soft soil.

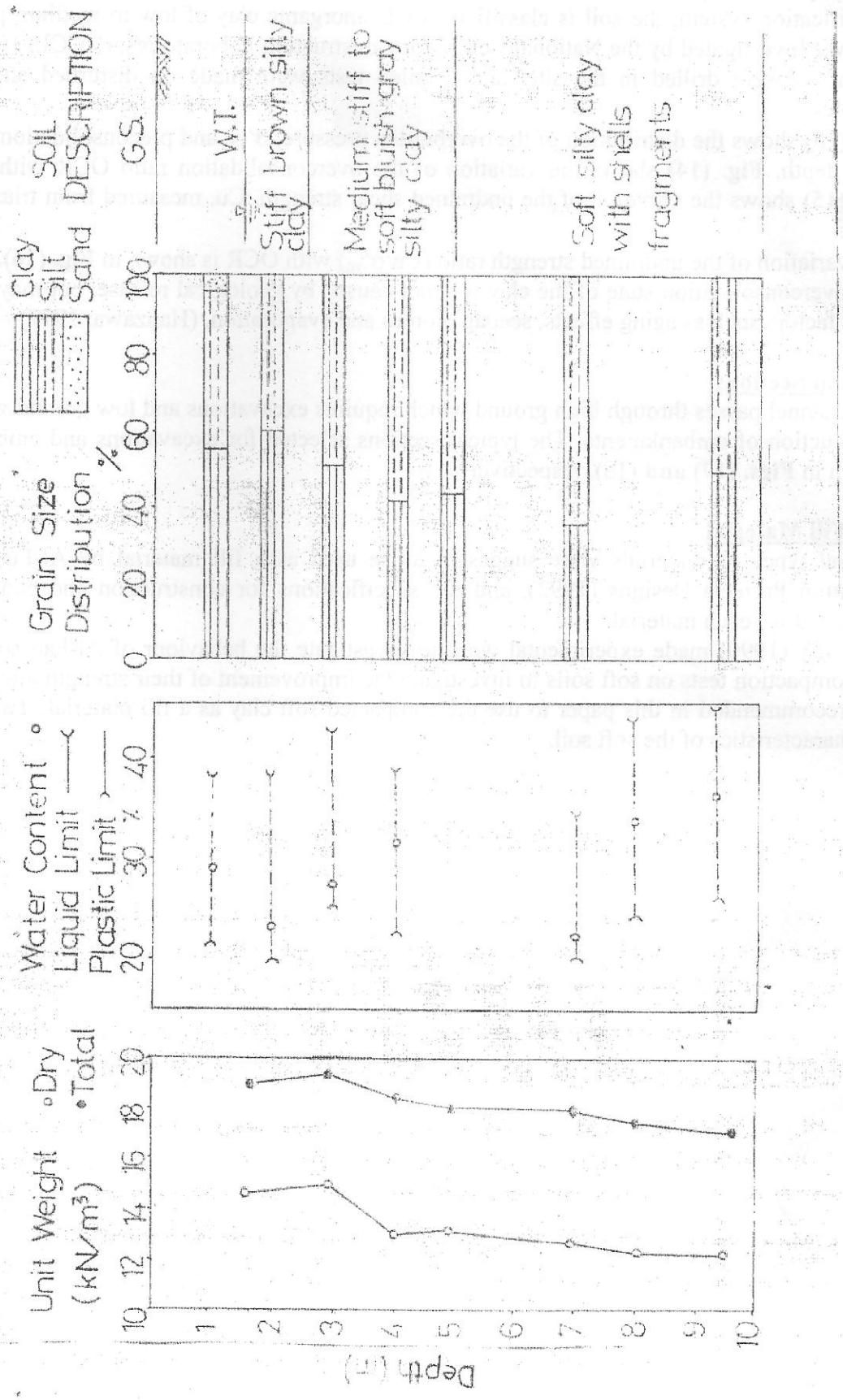

Fig. (12) – Physical properties of the soil profile.

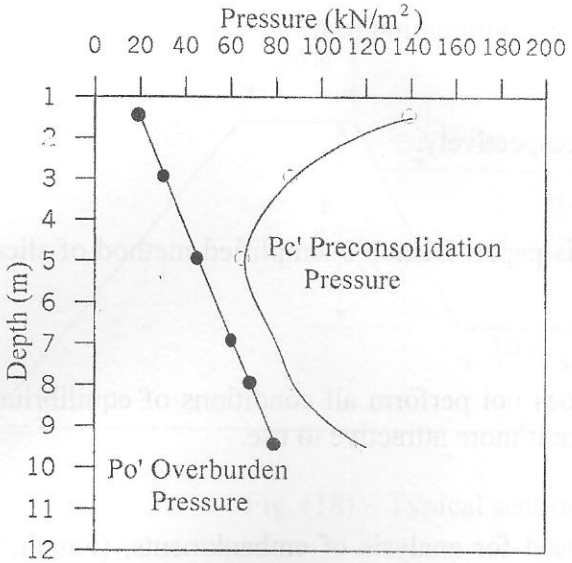

Fig. (13) - Distribution of overburden and preconsolidation pressure with depth, (after NCCL, 1992).

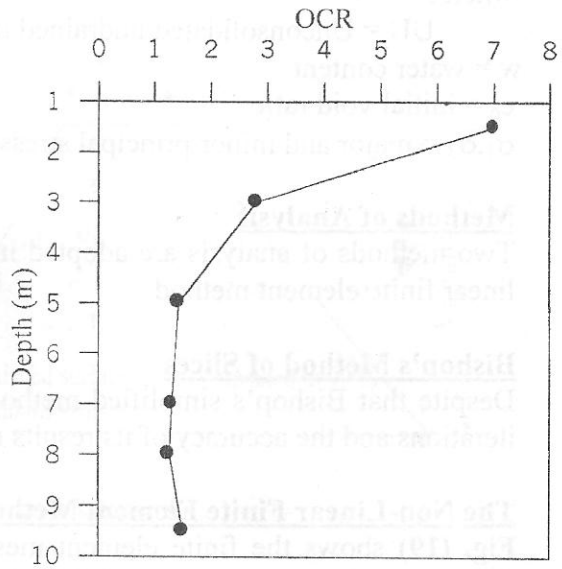

Fig. (14) - Distribution of overconsolidation ratio with depth.

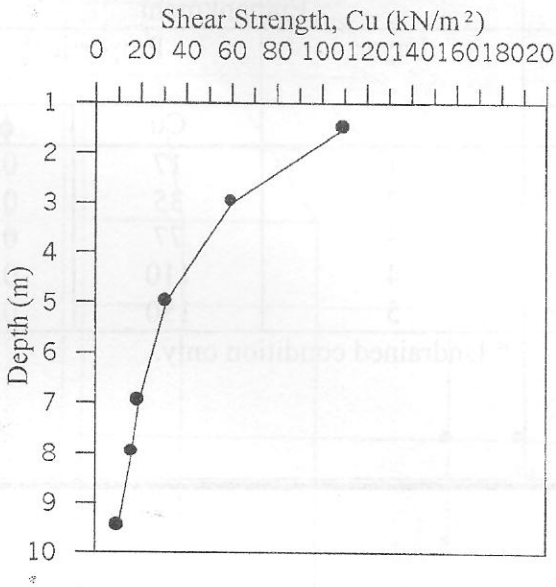

Fig. (15) - Variation of the undrained shear strength with depth, (after NCCL, 1992).

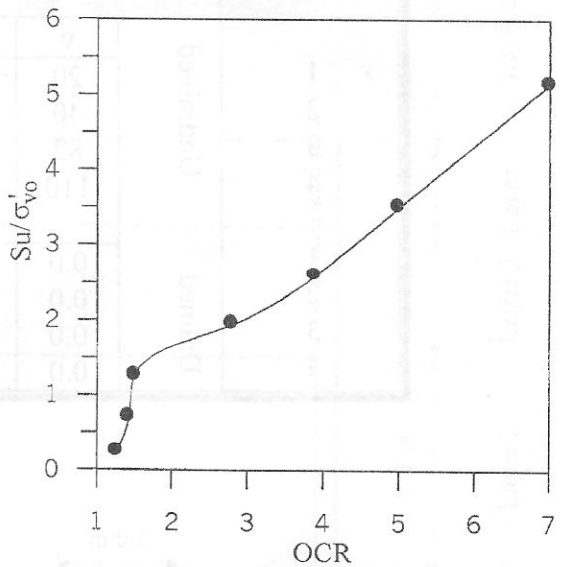

Fig. (16) - Normalized undrained strength (Su/σ'_{vo}) vs. OCR.

Table (1) – Results of strength tests on compacted clay used as a fill material, (after Al-Mufty, 1990).

Results of UU tests

Test	W (%)	e_o	σ_3 (kPa)	$(\sigma_1-\sigma_3)_f$ (kPa)	Cu (kPa)	$C_{uav.}$ (kPa)
1	20.5	0.681	100	277.0	138.5	
2	20.5	0.681	200	314.6	157.3	151.3
3	20.5	0.861	300	316.0	158.0	

where:

UU = Unconsolidated undrained triaxial compression test.

w = water content

e_o = initial void ratio

σ_1, σ_3 = major and minor principal stresses, respectively.

Methods of Analysis

Two methods of analysis are adopted in this paper: Bishop's simplified method of slices and non-linear finite element method.

Bishop's Method of Slices

Despite that Bishop's simplified method does not perform all conditions of equilibrium, the little iterations and the accuracy of its results make it more attractive to use.

The Non-Linear Finite Element Method

Fig. (19) shows the finite element mesh used for analysis of embankments, (Fattah, 1996). The shear strength parameters at each layer in the mesh are given in **Table (2).**

Table (2) – Shear strength parameters used in the analysis.

Excavation				Embankment		
Layer	Properties			Layer	Properties*	
		c	ϕ		Cu	ϕu
1	Undrained	20	0.0	1	17	0.0
2		40	0.0	2	35	0.0
3		82	0.0	3	77	0.0
4		110	0.0	4	110	0.0
				5	150	0.0
1	Drained	0.0	22	* Undrained condition only.		
2		0.0	28			
3		0.0	32			
4		0.0	39			

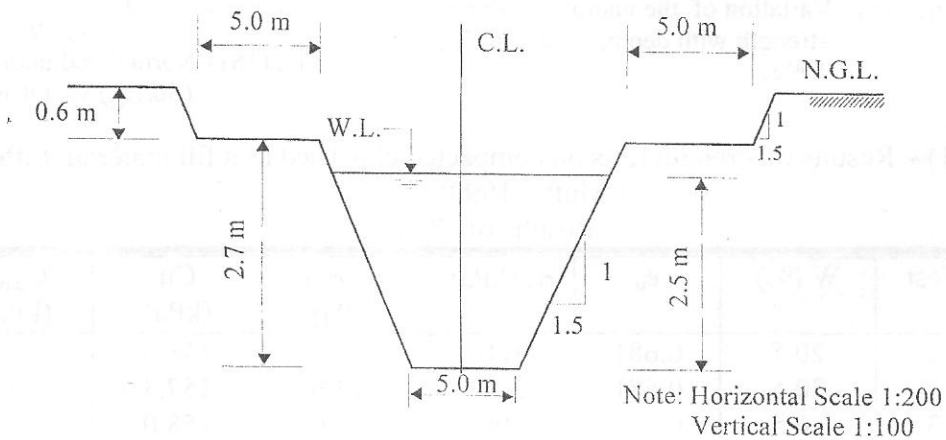

Fig. (17) – Typical section for excavation.

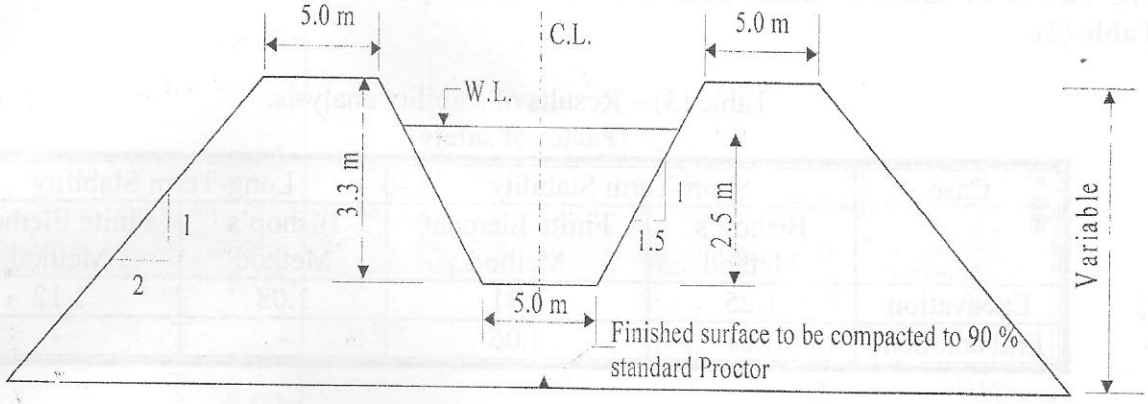

Fig. (18) – Typical section for embankment.

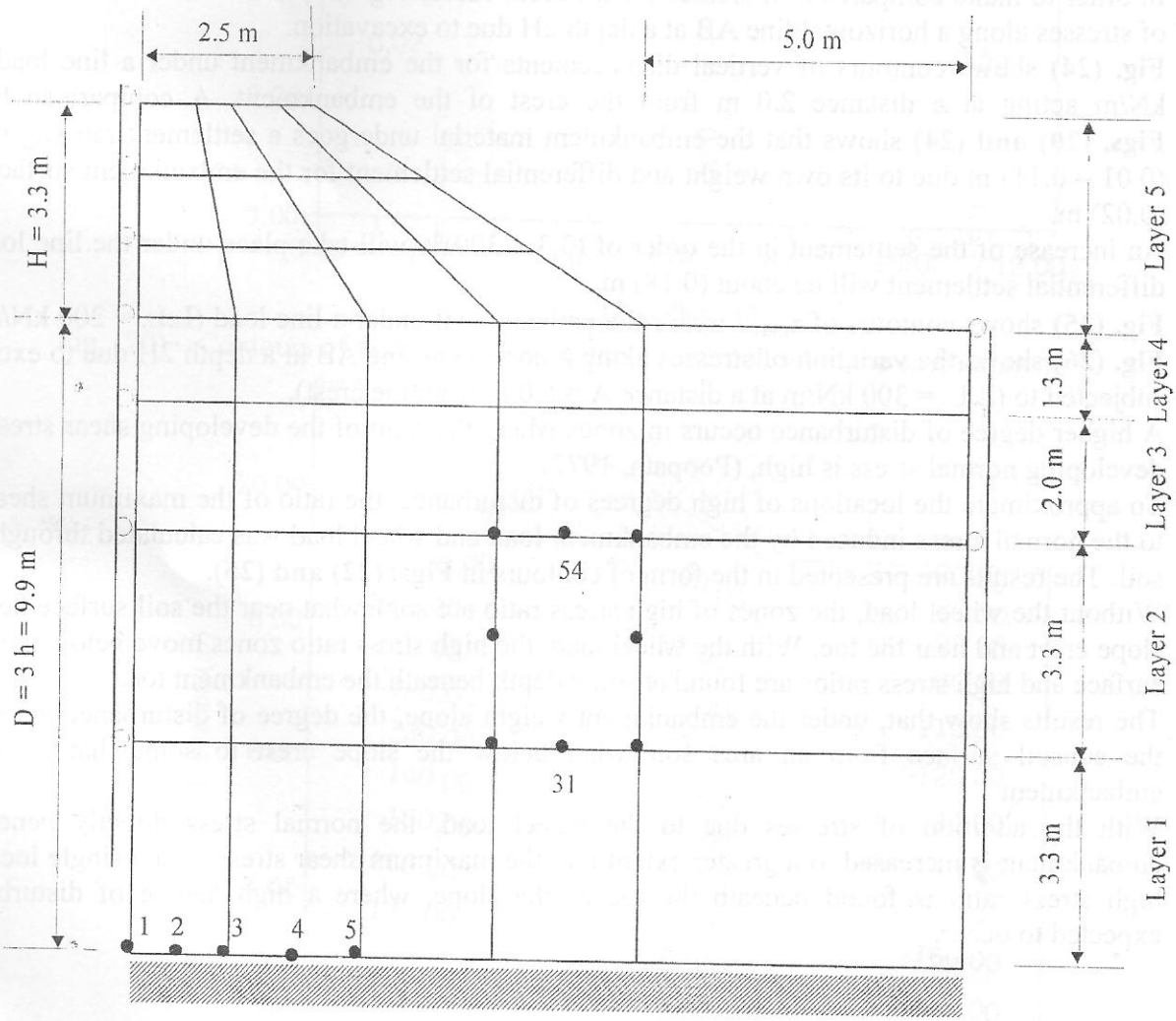

Fig. (19) – The finite element mesh for embankment.

Analysis Results

The factors of safety obtained from the stability analysis using the two methods are listed in **Table (3).**

Table (3) – Results of stability analysis.
(Factor of safety)

Case	Short-Term Stability		Long-Term Stability	
	Bishop's Method	Finite Element Method	Bishop's Method	Finite Element Method
Excavation	1.25	1.31	1.08	1.12
Embankment	3.81	4.06	-	-

Fig. (20) shows contours for vertical displacements (δv) in the embankment under gravity loading. **Figs. (21) and (22)** show contours of σ_1 and τ_{max}/σ_n (maximum shear stress/normal stress) in the embankment.

In order to make comparison of sresses for different cases, **Fig. (23)** is drawn to show the variation of stresses along a horizontal line AB at a depth 2H due to excavation.

Fig. (24) shows contours of vertical displacements for the embankment under a line load = 200 kN/m acting at a distance 2.0 m from the crest of the embankment. A comparison between **Figs. (20) and (24)** shows that the embankment material undergoes a settlement ranging between (0.01 – 0.11) m due to its own weight and differential settlement for the embankment surface about (0.02) m.

An increase of the settlement in the order of (3.3 – 300)% will take place under the line load. The differential settlement will be about (0.18) m.

Fig. (25) shows contours of τ_{max} / σ_n for the embankment under a line load (L.L. = 200 kN/m), and **Fig. (26)** shows the variation of stresses along a horizontal line AB at a depth 2H due to excavation subjected to (L.L. = 300 kN/m at a distance A = 6.0 m from the crest).

A higher degree of disturbance occurs in zones where the ratio of the developing shear stress to the developing normal stress is high, (Poopath, 1977).

To approximate the locations of high degrees of disturbance, the ratio of the maximum shear stress to the normal stress induced by the embankment load and wheel load was calculated throughout the soil. The results are presented in the form of contours in **Figs. (22) and (25).**

Without the wheel load, the zones of high stress ratio are somewhat near the soil surface below the slope crest and near the toe. With the wheel load, the high stress ratio zones move below the subsoil surface and high stress ratios are found at some depth beneath the embankment toe.

The results show that, under the embankment weight alone, the degree of disturbance is high near the subsoil surface from an area somewhat below the slope crest to somewhat outside the embankment.

With the addition of stresses due to the wheel load, the normal stress directly beneath the embankment is increased to a greater extent that the maximum shear stress, and a single location of high stress ratio is found beneath the toe of the slope, where a high degree of disturbance is expected to occur.

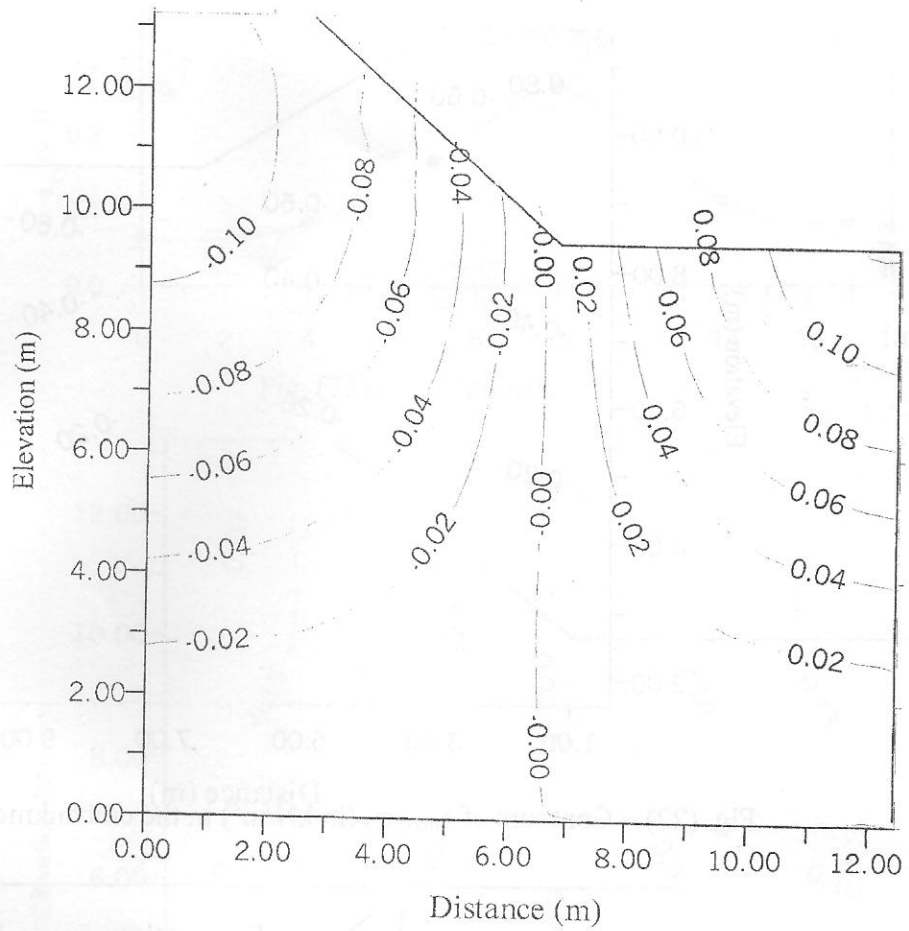

Fig. (20) – Contours of vertical displacements (δ_v in meters) in the embankment.

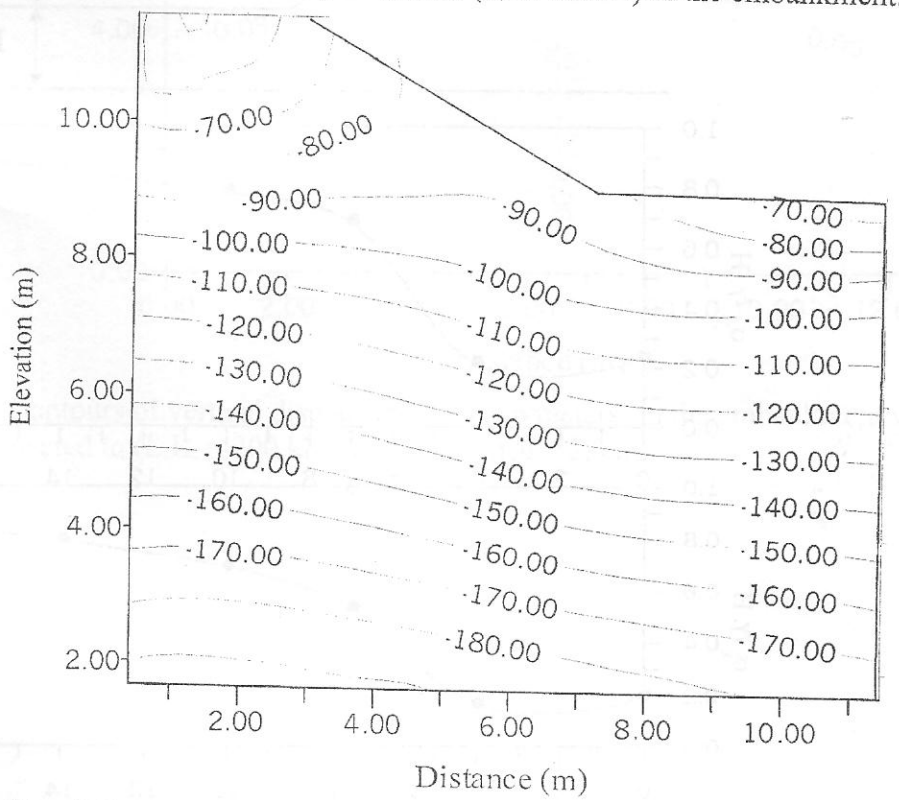

Fig. (21) – Contours of σ_1 (in kN/m^2) in the embankment.

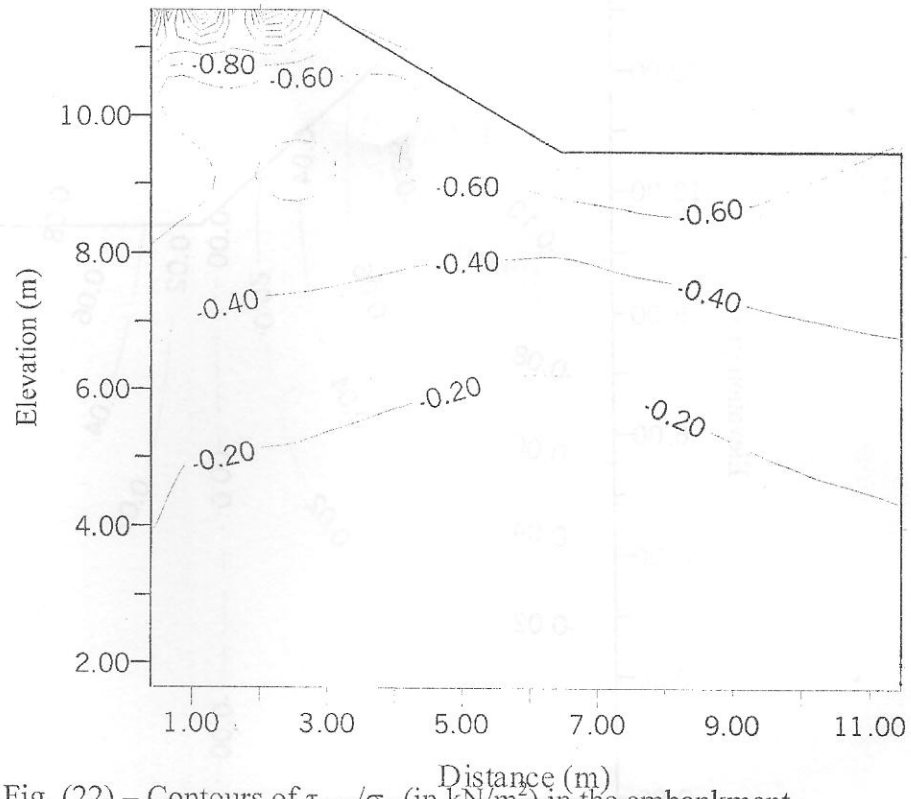

Fig. (22) – Contours of τ_{max}/σ_n (in kN/m^2) in the embankment.

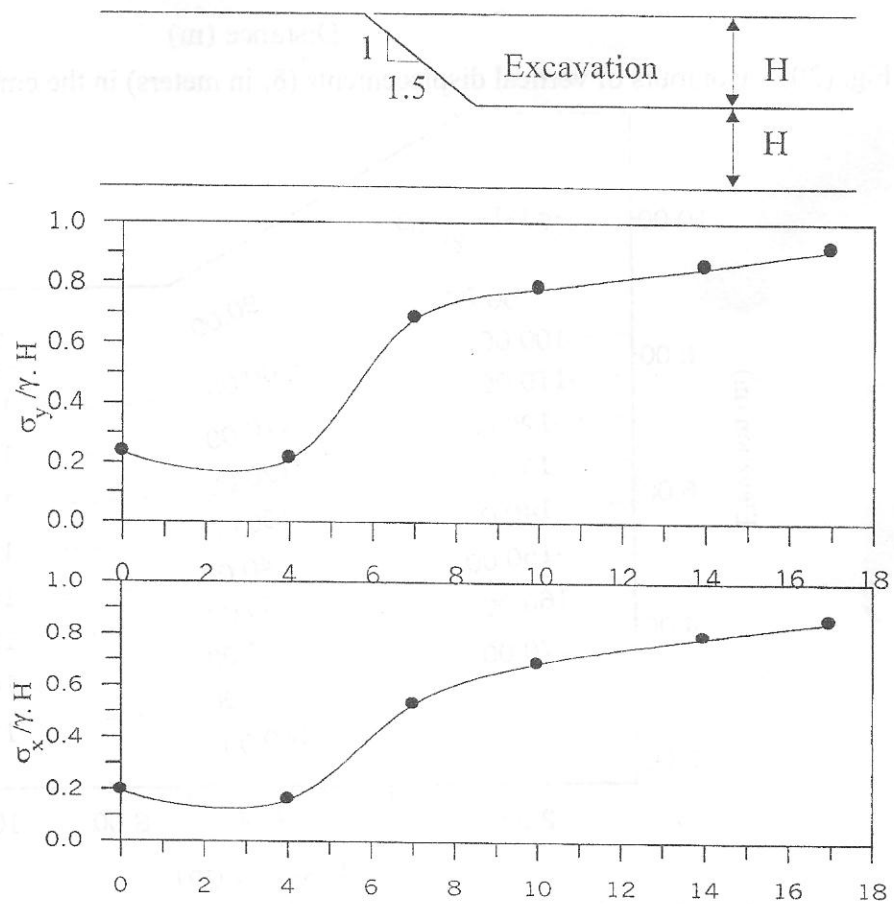

Fig. (23) – Stresses along a horizontal line at a depth 2H due to excavation.

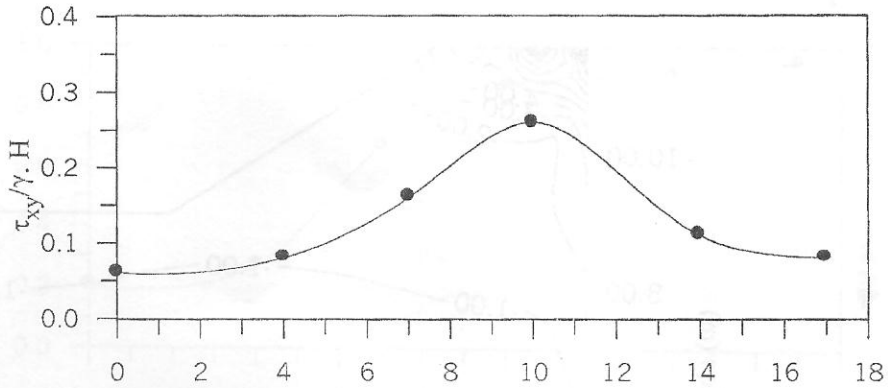

Fig. (23) – (Continued).

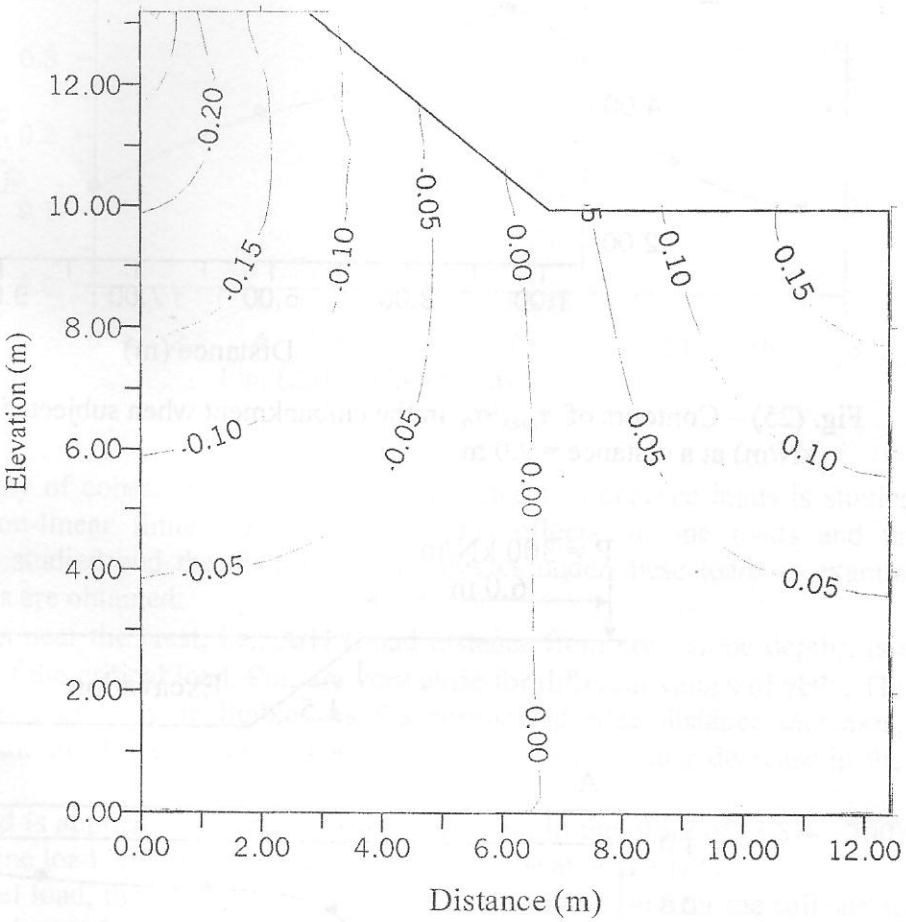

Fig. (24) – Contours of vertical displacements (δ_v in meters) in the embankment when subjected to (L.L. = 200 kN/m) at a distance = 2.0 m.

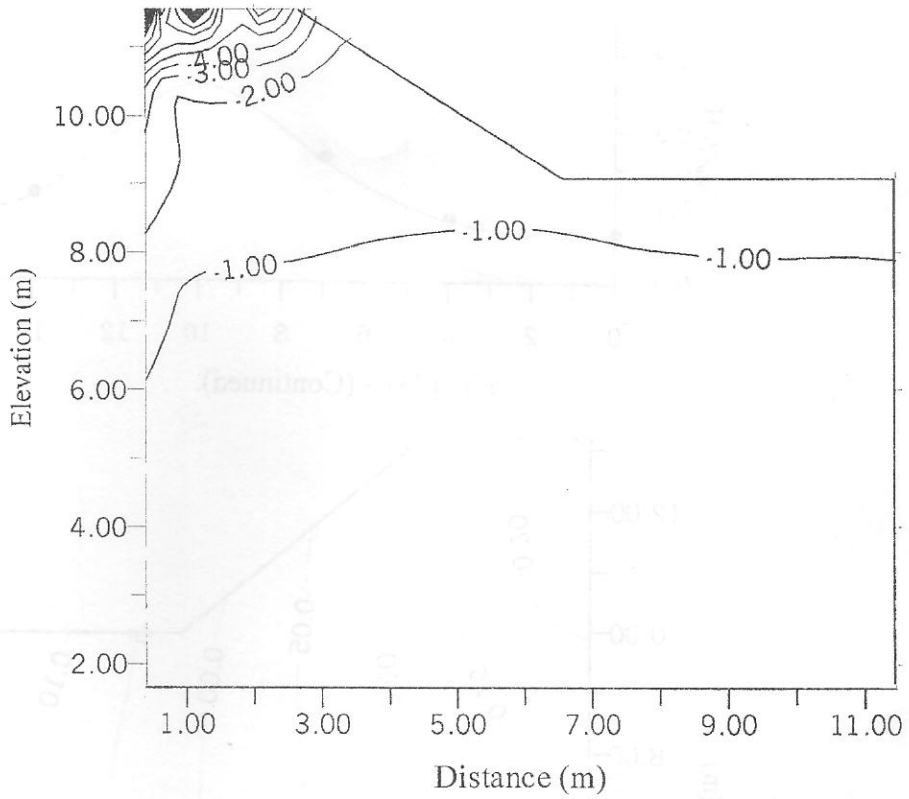

Fig. (25) – Contours of τ_{max}/σ_n in the embankment when subjected to (L.L. = 200 kN/m) at a distance = 2.0 m.

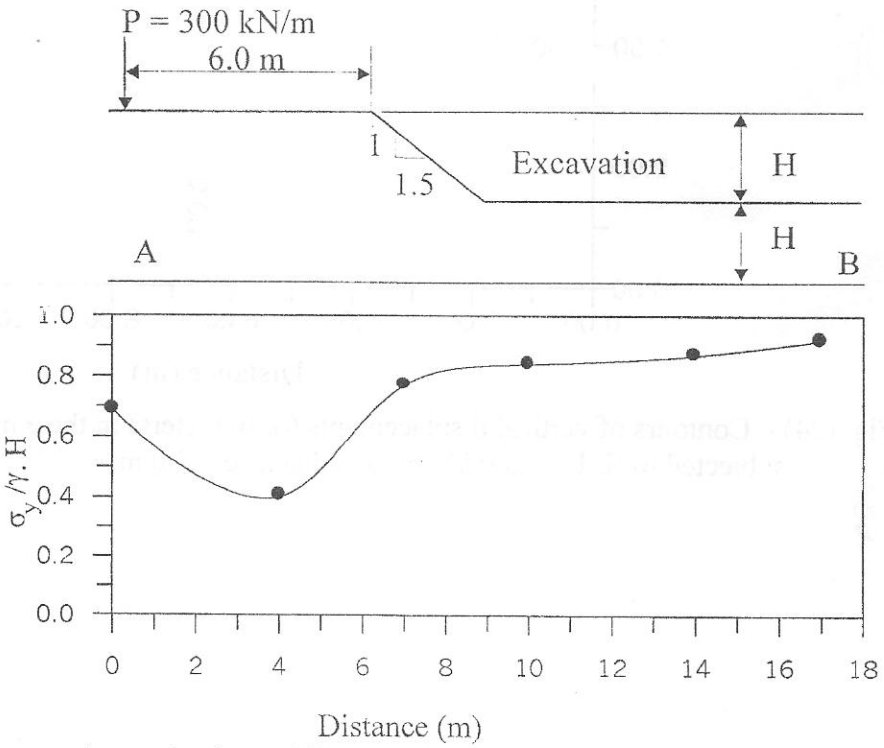

Fig. (26) – Stresses along a horizontal line at a depth 2H due to excavation subjected to line load = 300 kN/m at a distance = 6.0 m.

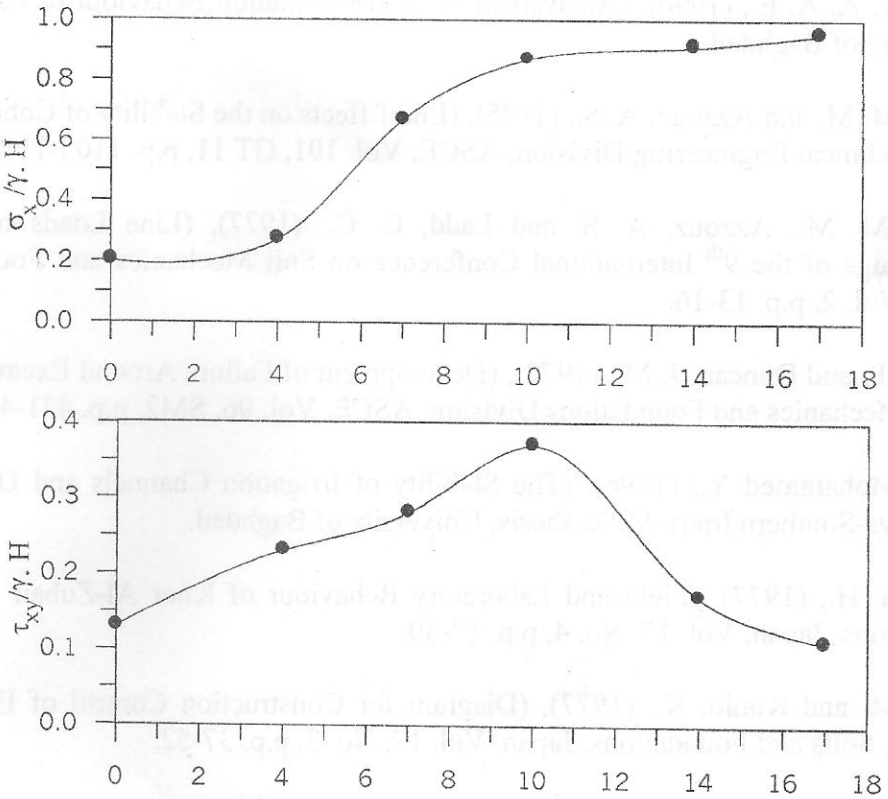

Fig. (26) – (Continued).

CONCLUSIONS

The undrained stability of cohesive slopes ($\phi_u = 0$) subjected to surcharge loads is studied in this paper. Using the non-linear finite element method, the effects of line loads and uniformly distributed loads are studied and the distribution of stresses under these loads is examined. The following conclusions are obtained:

1- When the load is near the crest, i.e., A/H (Load distance from crest/slope depth), is small ($\leq$ 0.2), the values of the critical load, Pcr, are very close for different values of $\gamma H/c$. This means that the effect of gravity is negligible. As the normalized edge distance increases, gravity becomes important and Pcr/cH increases with A/H because of greater decrease in the driving moment.

2- When a line load is applied, an increase of the settlement in the order of (3.3 – 300)% takes place under the line load. The differential settlement will be about (0.18) m.

3- Without the wheel load, the zones of high stress ratio are somewhat near the soil surface below the slope crest and near the toe. With the wheel load, the high stress ratio zones move below the subsoil surface and high stress ratios are found at some depth beneath the embankment toe.

4- The results show that, under the embankment weight alone, the degree of disturbance is high near the subsoil surface from an area somewhat below the slope crest to somewhat outside the embankment.

REFERENCES

Adikari, G. S. and Cummins, P. J., (1985), (An Effective Stress Slope Stability Analysis Method for Dams), Proceedings of the 11th ICSMFE, San Francisco, Vol. 2, p.p. 713-718.

Al-Furat Center for Irrigation Projects Designs, (1992), (Drawings and Specifications for Al-Basrah Water Supply Project).

Al-Mufty, A. A. E., (1990), (Analysis of Stress Deformation Behaviour of Fao Soil), M.Sc. thesis, University of Baghdad.

Baligh, M. M. and Azzouz, A. S., (1975), (End Effects on the Stability of Cohesive Slopes), Journal of Geotechnical Engineering Division, ASCE, Vol. 101, GT 11, p.p. 1105-1117.

Baligh, M. M., Azzouz, A. S. and Ladd, C. C., (1977), (Line Loads on Cohesive Slopes), Proceedings of the 9th International Conference on Soil Mechanics and Foundation Engineering, Tokyo, Vol. 2, p.p. 13-16.

Dunlop, P. and Duncan, J. M., (1970), (Development of Failure Around Excavated Slopes), Journal of Soil Mechanics and Foundations Division, ASCE, Vol. 96, SM2, p.p. 471-493.

Fattah, Mohammed Y., (1996), (The Stability of Irrigation Channels and Drains Constructed on Soft Clays-Southern Iraq), M.Sc. thesis, University of Baghdad.

Hanzawa, H., (1977), (Field and Laboratory Behaviour of Khor Al-Zubair Clay-Iraq), Soils and Foundations, Japan, Vol. 17, No. 4, p.p. 17-30.

Matsu, M. and Kunio, K., (1977), (Diagram for Construction Control of Embankments on Soft Ground), Soils and Foundations, Japan, Vol. 17, No. 3, p.p. 37-52.

NCCL, (1992), (Unpublished Soil Investigation Report on Al-Bassrah Water Supply Project), Iraq.

Poopath, V., (1977), (In Situ Strength and Total Stress Analysis for an Embankment on a Soft Foundation), Proceedings of the International Symposium on Soft Clay, Bangkok, p.p. 547-557.

Smith, I. M. and Griffiths, D. V., (1988), (Programming the Finite Element Method), second edition, John Wiley, New York.

Wright, S. G., Kulhawy, F. H. and Duncan, J. M., (1973), (Accuracy of Equilibrium Slope Stability Analysis), Journal of Soil Mechanics and Foundations Division, ASCE, Vol. 99, SM 10, p.p. 783-791.